IEEE Access
Multidisciplinary | Rapid Review | Open Access Journal

Received March 12, 2020, accepted April 1, 2020, date of publication April 6, 2020, date of current version April 22, 2020.

Digital Object Identifier 10.1109/ACCESS.2020.2985722

A New Design Methodology for Wideband Analog Predistorter With the Characteristics of Frequency-Dependent Gain and Phase Conversions

CHENGE BIAN, DEWEI ZHANG, HAILIN DENG, DALONG LV, AND YI ZHANG
National Digital Switching System Engineering and Technology Research and Development Center, Zhengzhou 450001, China
Corresponding author: Chenge Bian (bcg20140801@stu.xjtu.edu.cn)

ABSTRACT A novel design method, which can transform the nonlinear circuits design to the impedance matching network (IMN) design, is proposed for wideband analog predistoter (APD) with the characteristics of frequency-dependent gain and phase conversions in this paper. First, the design method for the desired gain and phase conversions is introduced. The ABCD parameters of the IMN can be computed. To simplify the design, the obtained parameters are transformed to the IMN terminal impedance. Then we can only need to design the IMN terminal impedance to obtain the desired transfer characteristics. In the meanwhile, an APD with 4.5 dB gain conversion and 50° phase conversion is designed and simulated to validate the design method for specify gain and phase conversions. The simulated results show good effectiveness of the design method. Second, for wideband application, the complex gain and phase conversions surface design is transformed to the IMN terminal impendence curve versus frequency design. This gives the designers a well-defined strategy for wideband APD design focusing on frequency-dependent phase conversion as well as gain conversion. To validate the proposed method, a wideband APD operating at K-band (17-20 GHz) is designed, fabricated and measured. A linearized 100W K-band TWTA is shown to achieve a noise power ratio (NPR) >20 dB at 3 dB output power back-off, and phase change <6.5° among the operating band.

INDEX TERMS Wideband analog predistorter, impedance matching network, terminal impedance.

I. INTRODUCTION

The demand for higher information rates has resulted in more complex digital modulation which has the characteristic of high peak-to-average power ratio (PAPR). Therefore, requirements of the high power amplifier (HPA) with high linearity have been becoming more critical. Normally HPA devices like traveling-wave tube amplifiers (TWTAs)/solid-state power amplifiers (SSPAs) should make a trade-off between linearity and efficiency. When the output power approaches the saturation point, the TWTAs will generate strong nonlinear distortion, which appears to gain compression and phase shift. Therefore, different linearization methods such as feedforward, feedback, analog predistortion and digital predistortion technique [1] are widely employed to improve the linear characteristics of TWTAs.

The associate editor coordinating the review of this manuscript and approving it for publication was Feng Lin.

Owing to its relative simplicity, wideband operation, and high efficiency, analog predistortion is widely used in microwave and millimeter wave systems [2]–[10]. The need for greater data rates promotes the move to operating over wider bandwidths and at higher frequency. For wideband applications, the linearizer's amplitude modulation (AM)/AM and AM/phase modulation (PM) conversions characteristics must change over frequency to match the changes of the PA's nonlinearity at different frequencies. Additional time delay, based on an artificial left-handed transmission line, is introduced to characterize the frequency-dependent phase conversion function [3]. But the circuit design is complicated and the gain conversion is not mentioned. In [4], Q-band (43.5-45.5 GHz) and V-band (47-52 GHz) APDs have been proposed for using with satellite communications (SATCOM) ground station TWTAs. But this paper lacks of technical information concerning the APD solution. Therefore, the clear design method of wideband

APD focusing on frequency- dependent gain and phase conversions have not be reported in the previous work.

In this paper, a new design method for the APD with specify gain and phase conversions is introduced. This method can transform the complex nonlinear circuits design to the IMN terminal impendence design. Then an APD with 4.5 dB gain conversion and 50° phase conversion is designed and simulated using the proposed method. The simulated results show good effectiveness. The design principle of wideband APD, which transfer characteristics varying with frequency, is to design the IMN terminal impendence curve versus frequency. Finally, a wideband APD is fabricated and measured. The measured results show good consistency with the analysis.

This paper is organized as follows. First, a design method for specify gain and phase conversions is presented in Section II. Based on the method, an APD with 4.5 dB gain conversion and 50° phase conversion is designed and simulated. Then the design procedure, simulation results and experiment results for wideband APD are provided in Section III. Finally, section IV draws the conclusion.

II. DESIGN METHOD FOR SPECIFY GAIN AND PHASE CONVERSIONS

A. DESIGN METHOD

A variable impedance matching network based on varactor diode is introduced in [8] to achieve the tuning function by changing its bias voltage. But it does not give a well-defined matching network design strategy for the desired gain and phase conversions. Further analysis on the IMN design strategy is given below. The topology of the APD is shown in Fig. 1, which consists of a 90° hybrid coupler, two IMNs, two resistances and two nonlinear loads (Schottky diode). Based on Ref. [11], the gain G and phase shift Φ of the APD can be derived:

$$G = 20\lg|\Gamma| \tag{1}$$

$$\Phi = \Phi_\Gamma + 90^\circ \tag{2}$$

where Γ is the reflection coefficient of a wave incident on the load, from the through or coupled port of the 90° hybrid.

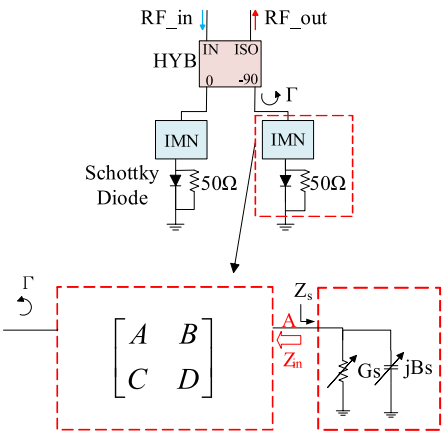

FIGURE 1. The topology of the APD.

As shown in Fig. 1, the Schottky diode and the resistance can be equivalent to a parallel nonlinear capacitor and a parallel nonlinear resistor, and its equivalent susceptance *Bs* and conductance *Gs* are both the function of input power. For a reciprocity network, the transmission matrix of the IMN can be expressed as:

$$[T] = \begin{bmatrix} A & B \\ C & D \end{bmatrix} \tag{3}$$

and it meet the following conditions:

$$AD - BC = 1 \tag{4}$$

Then the transmission matrix after through port of hybrid coupler can be derived as:

$$[T'] = \begin{bmatrix} A & B \\ C & D \end{bmatrix} \begin{bmatrix} 1 & 0 \\ G + jB_s & 1 \end{bmatrix} = \begin{bmatrix} A + BG + jBB_s & B \\ C + DG + jDB_s & D \end{bmatrix} \tag{5}$$

and the output impedance of the through port of hybrid coupler can also be derived from the transmission matrix $[T']$:

$$Z = \frac{D}{C + DG + jDB_s} \tag{6}$$

Assume the impedance of the through port of hybrid coupler is Z_0, then the reflection coefficient can be derived as:

$$\Gamma = \frac{Z - Z_0}{Z + Z_0} \tag{7}$$

According to (3) - (7), we can easy to obtain that the gain and phase shift vary with the input power and the circuit parameters of IMN. The principle of the APD can be described as follows: when the circuit topology and the circuit parameters of IMN are determined, the gain and phase shift only vary with the input power. Then the gain conversion ΔG and phase conversion $\Delta\Phi$ can be further derived as:

$$\Delta G = 20\lg|\Gamma_h / \Gamma_l| \tag{8}$$

$$\Delta\Phi = \Phi_{\Gamma_h} - \Phi_{\Gamma l} \tag{9}$$

where Γ_h and Γ_l are the reflection coefficient at the highest and lowest input power, respectively.

According to (8) and (9), the gain and phase conversions can be calculated, so we can tune the value of Γ_h and Γ_l to get the desired gain and phase conversions. When the Schottky diode model is chosen, the equivalent conductance *Gs* and susceptance *Bs* of the Schottky diode and the resistance in different input power are determined. The circuit parameters can be calculated by (3) - (9) for specify gain and phase conversions. Because the solution is not unique, so we should choose the solution which can minimize the insertion loss (IL) in order to decrease the power consumption. The IL can be derived as:

$$IL = -20\lg\left(\frac{Z - Z_0}{Z + Z_0}\right) \tag{10}$$

Finally, the problem can be derived as:

$$\min f = IL \quad s.t. \begin{cases} \Delta G = a \\ \Delta \Phi = b \\ AD - BC = 1 \end{cases} \tag{11}$$

where a and b are the specify gain and phase conversions, respectively.

We use the genetic algorithm to solve above problem, then the ABCD parameters can be obtained. However, although these parameters can represent the characteristics of the IMN, but they are more complicated to apply in practical circuits design. To simplify the design, we transform the ABCD parameters to the terminal impedance Z_{in} at port A. Then Z_{in} can be derived as:

$$Z_{in} = \frac{Z_0 D}{Z_0 C + D} \tag{12}$$

From above analysis, the specify gain and phase conversions design are transformed to the terminal impedance of the IMN design.

B. AN APD WITH 4.5 dB GAIN CONVERSION AND 50° PHASE CONVERSION

A design method for APDs with specify gain and phase conversions is introduced in section A. the flowchart of the design procedure is shown in Fig. 2. To validate the proposed design method, an APD with 4.5 dB gain conversion and 50° phase conversion is designed and simulated using the design methodology. An APD operating at 49 GHz is simulated using Rogers 5880 with a relative dielectric constant of 2.2 and a thickness of 10 mil. DBES105a Schottky diode is adopted in this circuit. From the prior analysis, the design procedure follows:

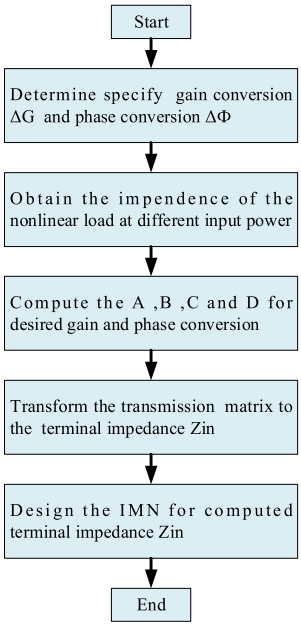

FIGURE 2. Flowchart of the design procedure.

a) *Step 1*: Give the specify gain and phase conversions(4.5 dB and 50°), operating frequency(49 GHz) and the Schottky diode(DBES105a).

b) *Step 2*: Obtain the *Gs* and *Bs* at different input power. First, the impedance of the Schottky diode and the resistance (*Zs*) can be simulated by the Advanced Design System (ADS). The setup of the simulation is shown in Fig. 3. Then the impedance can be obtained using the Zin toolbox. Fig. 4 shows the simulated impedance versus input power, then *Gs* and *Bs* at different input power can be derived:

$$Z_s = 1/(G_s + jB_s) \tag{13}$$

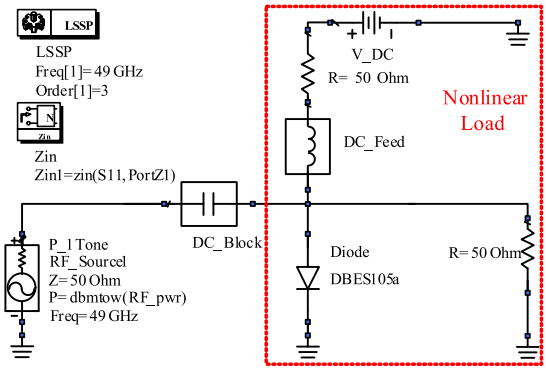

FIGURE 3. The setup of the Gs and Bs simulation.

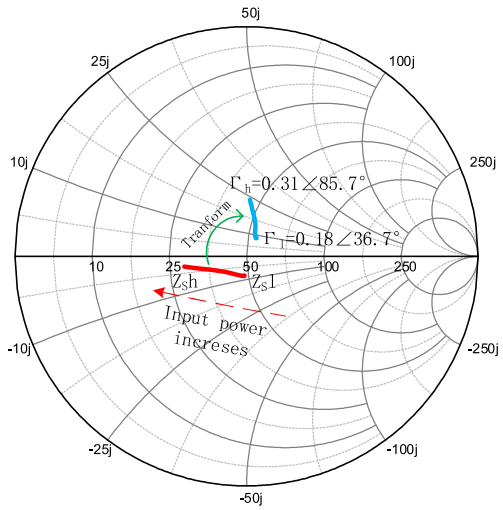

FIGURE 4. The simulated impedance Zs and the reflection coefficient Γ at different input power (where Zsh and Zsl are the impedance of the Schottky diode and the resistance at the highest and lowest input power, respectively.).

c) *Step 3*: According to (1) - (11), the ABCD parameters can be obtained using the genetic algorithm. The calculated parameters are: $A = 1.029$, $B = -\text{j}0.287$, $C = -\text{j}0.011$ and $D = 1.033$. Then these parameters

are transformed to terminal impedance of the IMN: $Z_{in} = 39.73 + 22.98j$.

d) *Step 4*: Then the specify gain and phase conversion design can be transformed to the terminal impedance of the IMN design. The terminal impedance Z_0 (here we set $Z_0 = 50\ \Omega$) should be transformed to Z_{in} using the IMN. The Smith Chart toolbox is used to guide the IMN design, the details of the IMN is shown in Fig. 5.

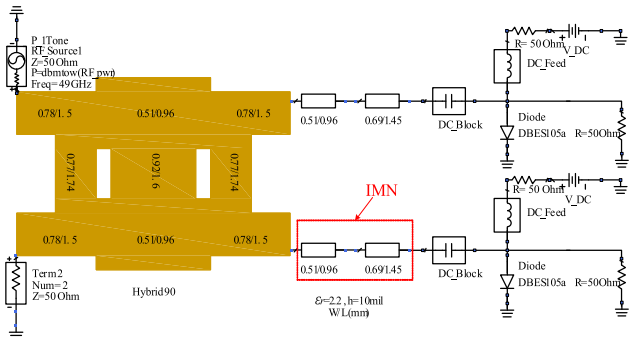

FIGURE 5. The Schematic of the designed APD.

As shown in Fig. 4, the function of the IMN is to transform the reflection coefficient to meet the specify gain and phase conversions' requirement. In the prior, a well-defined matching network design strategy is introduced for the specify gain and phase conversions' design.

The Schematic of the designed APD with 4.5 dB gain conversion and 50° phase conversion is shown in Fig. 5. A broadband three-branch hybrid coupler is adopted to achieve a better consistency within 47-51 GHz and the circuit parameters are shown in Fig. 5. Then the gain and phase conversions can be simulated by the ADS and the simulated results are shown in Fig. 6. The simulated gain and phase conversions are 4.36 dB and 48.5°, respectively. These results are very close to the given conversions showing good effectiveness of the design method for specify gain and phase conversions.

According to (8) – (9) and the simulated impedance of the Schottky diode, we can also calculate the gain and phase conversions. The calculated results are shown in Fig. 6. The gain and phase conversions are 4.51 dB and 51°, respectively.

The simulated and calculated results are close and the discrepancies between simulated and calculated results are mainly because the non-idealities of the hybrid coupler. For example, the impedance of the through port of hybrid coupler is not 50 Ω resulting in inaccurate results in (7) and (10).

III. A WIDE BAND APD FOR 100W K-band TWTA

A. DESIGN METHOD FOR WIDEBAND APD

In prior analysis, a design method for the APD with specify gain and phase conversions is introduced. However, a APD's design in wideband application is not to generate a special curve versus input power but also a surface with frequency and input power as variables. The main reason is that the needed gain and phase conversions in wideband application

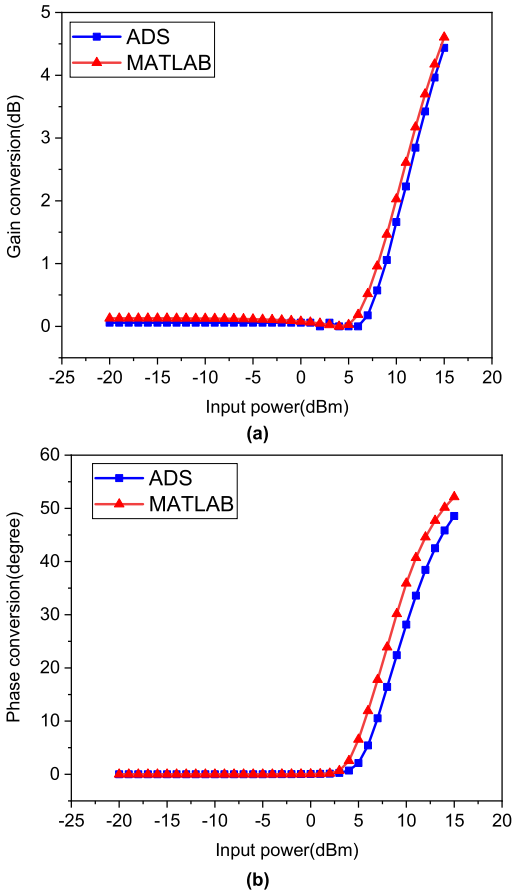

FIGURE 6. The simulated and calculated results of the designed APD (a) gain conversion and (b) phase conversion.

are frequency dependent. First, the wideband capability of the APD proposed in section II is analyzed. Second, a design method for wideband APD is introduced. Finally, a wideband APD operating at K-band (17-20 GHz) is designed, fabricated and measured.

Fig. 7 shows the simulated one-tone AM/AM and AM/PM conversions versus input power and frequency of the APD designed in section II. As shown in Fig. 7 (a), the gain conversion is 5.9, 4.3 and 2.4 dB at 47, 49 and 51 GHz, respectively. The gain conversion in low and high frequencies cannot meet the requirement of actual TWTAs. The phase conversion shown in Fig. 7 (b) is 42.5, 53.2 and 58.3 dB at 47, 49 and 51 GHz, respectively. The phase conversion in low frequency is larger than the needed. So the design method for specify gain and phase conversions cannot be directly used to design wideband APDs. In order to better analyze the relationship between the gain and phase conversions and the IMN terminal impedance, we fix one conversion and the other conversion is scanned (for constant-gain conversion situation, we set $\Delta G{=}a$, and let $\Delta\Phi$ varying from $-180°$ to 180°; for constant-phase conversion situation, we set $\Delta\Phi{=}b$, and let ΔG varying from -10 dB to 10 dB). Finally, constant-gain conversion and constant-phase conversion curves can be obtained. The function of these curves

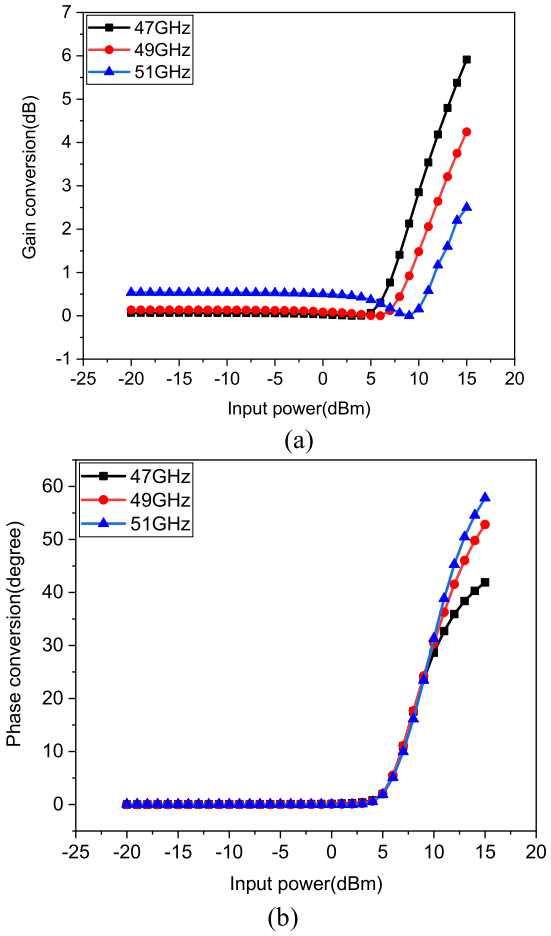

FIGURE 7. The simulated one-tone AM/AM and AM/PM conversions versus input power and frequency of the APD designed in section II (a) gain conversion and (b) phase conversion.

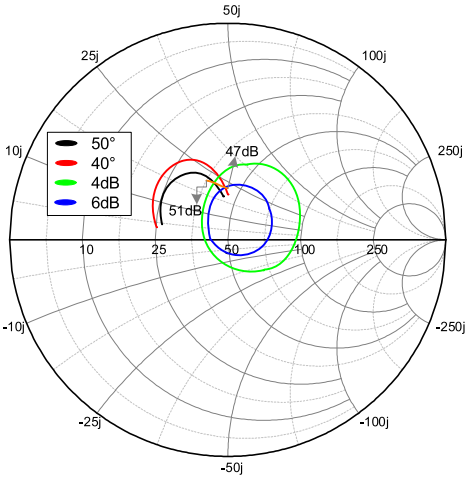

FIGURE 8. The constant-gain conversion and constant-phase conversion curves for the APD designed in section II.

are similar to the equal gain and equal efficiency curves in the power amplifier design, and can be easily used to guide the design. In the power amplifier design, the load-pull data (equal gain and equal efficiency curves) gives the designers a well-defined strategy for suitable matching network design. In our work, constant-gain conversion and constant-phase conversion curves gives IMN design target for specify gain and phase conversions. The Fig. 8 shows the constant-gain conversion and constant-phase conversion curves for the APD designed in section II.

Measured impedance of the Schottky diode and the resistance (Zs) is shown in Fig. 9. We can see that DBES105a Schottky diode with the nonlinear characteristics varys little in the operating band (17 GHz – 20GHz). So we can think that Gs and Bs are constant versus frequency in the operating band and assume that the admittance of the through port of hybrid coupler Y_0 vary little with frequency. From (3) - (6) we can see: constant-gain conversion and constant-phase conversion curves at all frequencies among operating band are equal.

To obtain a design method for wideband operation, we first analyze the terminal impedance curve versus frequency.

The transmission matrix of the two series transmission lines can be expressed as:

$$[T''] = \begin{bmatrix} \cos\beta\theta_1 & jZ_1\sin\beta\theta_1 \\ \dfrac{j\sin\beta\theta_1}{Z_1} & \cos\beta\theta_1 \end{bmatrix} \begin{bmatrix} \cos\beta\theta_2 & jZ_2\sin\beta\theta_2 \\ \dfrac{j\sin\beta\theta_2}{Z_2} & \cos\beta\theta_2 \end{bmatrix} \tag{14}$$

So the ABCD parameters is:

$$\begin{aligned} A &= \cos\beta\theta_1\cos\beta\theta_2 - \frac{Z_1}{Z_2}\sin\beta\theta_1\sin\beta\theta_2 \\ B &= jZ_2\cos\beta\theta_1\sin\beta\theta_2 + jZ_1\sin\beta\theta_1\cos\beta\theta_2 \\ C &= \frac{j\cos\beta\theta_1\sin\beta\theta_2}{Z_1} + \frac{j\sin\beta\theta_1\cos\beta\theta_2}{Z_2} \\ D &= \cos\beta\theta_1\cos\beta\theta_2 - \frac{Z_2}{Z_1}\sin\beta\theta_1\sin\beta\theta_2 \end{aligned} \tag{15}$$

Then we can obtain the terminal impedance curve versus frequency according to (12). The terminal impedance curve varying with frequency is shown in Fig. 8. The terminal impedance curve shows good consistency with the simulated one-tone AM/AM and AM/PM conversions shown in Fig. 7. Then the needed gain and phase conversions surface design is transformed to the specify terminal impedance curve versus frequency.

The design procedure follows: First, obtain the impedance of Schottky diode and resistance at different input power. Second, compute the terminal impedance for specify gain and phase conversions from (3) -(12) and plot the constant-gain conversion and constant-phase conversion curves. Third, according to the needed gain and phase conversions surface, choose a specify curve from constant-gain conversion and constant-phase conversion curves. Finally, design the IMN to meet the specify terminal impedance curves versus frequency.

B. SIMULATION

In this section, a wideband APD operating at K-band (17-20 GHz) is designed and simulated using the proposed

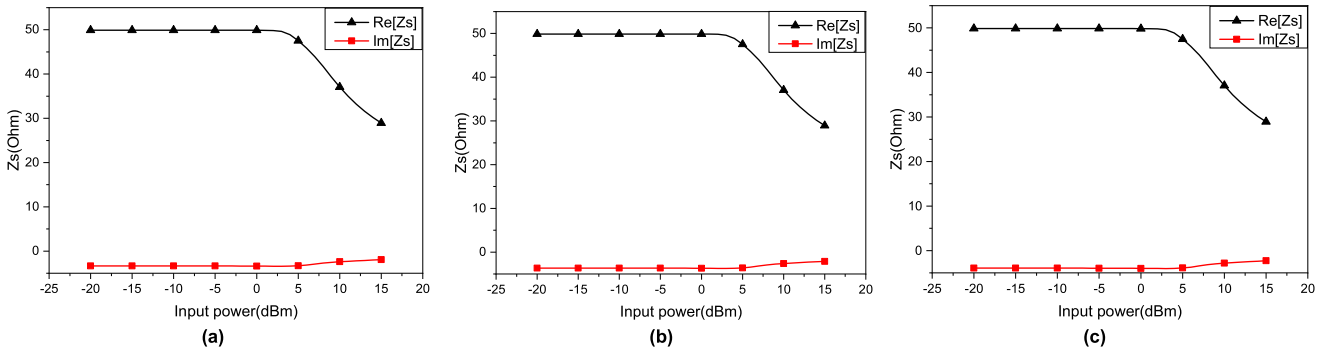

FIGURE 9. The constant-gain conversion and constant-phase conversion curves for the wideband APD.

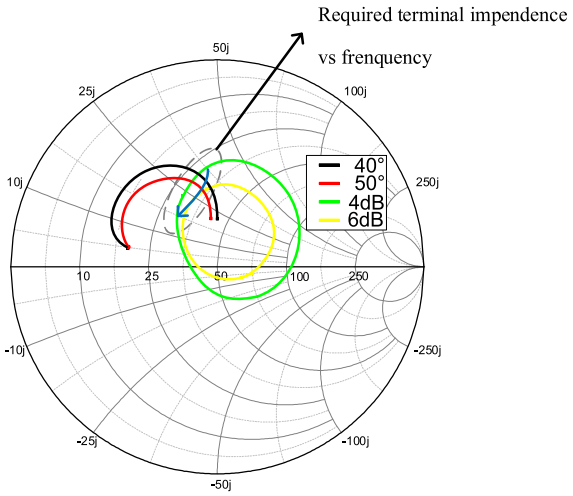

FIGURE 10. Measured impedance of the Schottky diode and the resistance (Zs) (a) 17GHz, (b) 18.5GHz and (c) 20GHz.

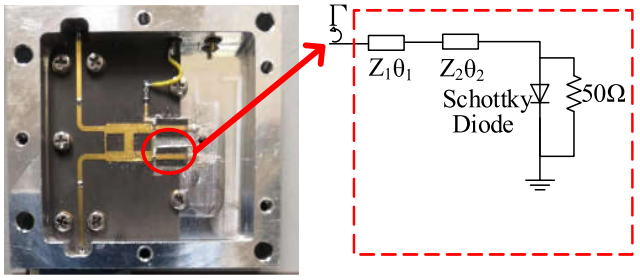

FIGURE 11. The fabricated wideband APD (Z1=45 Ω, θ98=°, Z2=80 Ω, θ20=° at center frequency).

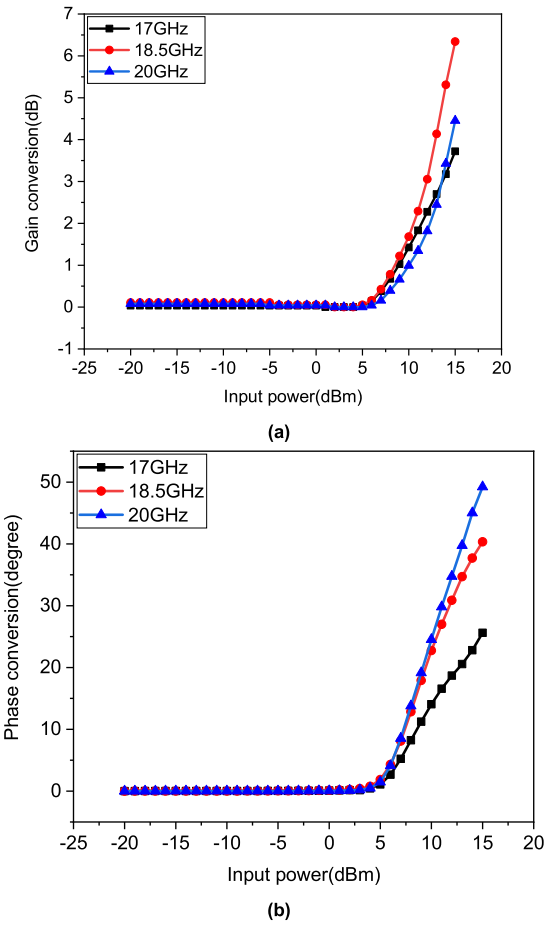

FIGURE 12. Simulated one-tone AM/AM and AM/PM conversions versus input power and frequency of the wideband APD (a) gain conversion and (b) phase conversion.

design method. Fig. 10 shows the constant-gain conversion and constant-phase conversion curves in K-band (17-20 GHz). In the wideband application, we should choose one curve to meet the requirement over the operating frequency band. For a specify 100 W K-band TWTA, the needed transfer response is: the gain conversion increases first and then decrease with frequency, and the phase conversion increases with frequency. Then the required curve is plotted in Fig. 10.

The detailed schematic and circuit parameters of the proposed IMN for the required specify curve is shown in Fig. 11. Fig. 12 shows the simulated one-tone AM/AM and AM/PM conversions versus input power and frequency of the wideband APD. The gain conversion is 3.7, 6.21 and 4.63 dB as well as the phase conversion is 26.1, 42.6 and 54.5 degrees at 17, 18.5 and 20 GHz, respectively. These results can meet the requirement of the 100 W K-band TWTA.

C. EXPERIMENTS

To validate the proposed method, a wideband APD is fabricated using Rogers 5880 with a relative dielectric constant of 2.2 and a thickness of 10 mil. DBES105a Schottky diodes is adopted in this circuit. Moreover, we implement a broadband three-branch hybrid coupler to achieve a better consistency within 17-20 GHz, and set the through port impedance $Z_0 = 50\ \Omega$. The fabricated wideband APD is shown in Fig. 10.

Fig. 13 shows the measured one-tone AM/AM and AM/PM conversions performance of the proposed APD, the gain conversion is 3.8, 6.1 and 4.5 dB as well as the phase conversion is 25, 43 and 55 degrees at 17, 18.5 and 20 GHz, respectively. The transfer response versus input power and frequency show very good consistency with the above analysis and the simulated results.

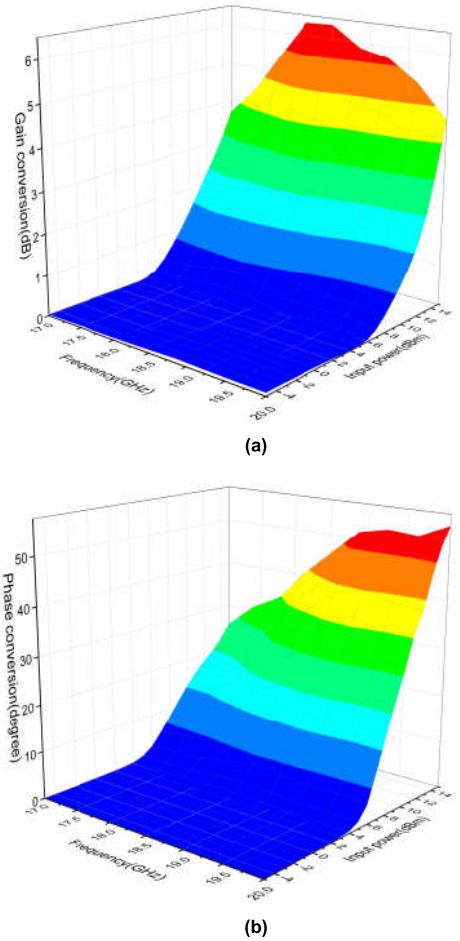

FIGURE 13. Measured one-tone AM/AM and AM/PM conversions versus input power and frequency of the wideband APD (a) gain conversion and (b) phase conversion.

To validate the performance of the linearizer, a 100 W K-band TWTA is selected. The experimental setup is shown in Fig. 14. A linear driver power amplifier is cascaded in the front of the proposed APD to make sure APD working

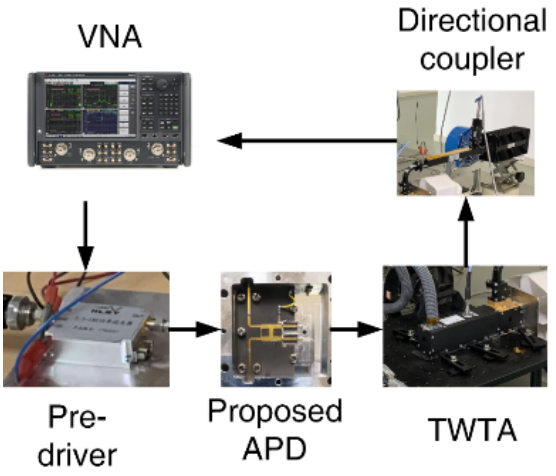

FIGURE 14. Experimental setup.

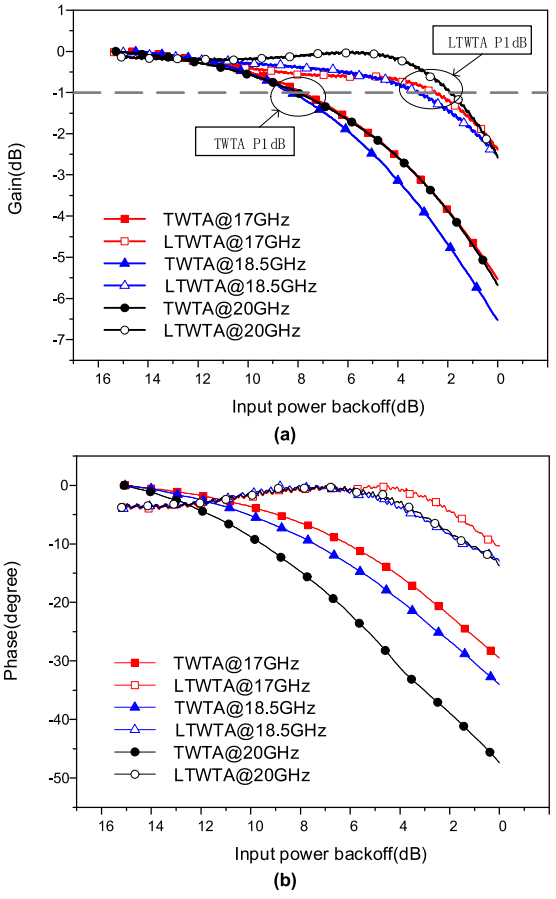

FIGURE 15. Measured gain and phase conversions of the TWTA and LTWTA (a) gain conversion and (b) phase conversion.

in appropriate power range. Agilent N5244A PNA-X vector network analyzer (VNA) is applied in the measurement.

Fig. 15 shows the measured gain and phase conversions of the TWTA and linearized TWTA(LTWTA). Linearization moves the 1-dB compression point of the TWTA to within 2.5 dB in input power (0.6 dB output power) from saturation point. The measured phase conversion of the

TABLE 1. Comparison with other reported wideband APDS.

	Freq.(GHz)	Phase conversion versus freq.(degree)	The change in phase after linearized (degree)	C/IM3 of the linearized PAs(dBc)	DUT	Structure
[3]	20 to 21.5	12.9 to 30.8	Not mentioned	Not mentioned	Not mentioned	Complex: predistortion linearizer model with LHTL time delay
[4]	43.5 to 45.5	33 to 57	<10	>26 @3 dB OBO	Q-band TWTA	Not mentioned
[7]	17.3–20.2	25 to 60	<5.5	Not mentioned	170W K-band TWTA	complex: vector combination
This	17 to 20	25 to 53	<6.5	26.7 @3 dB OBO	100W K-band TWTA	simple: reflective

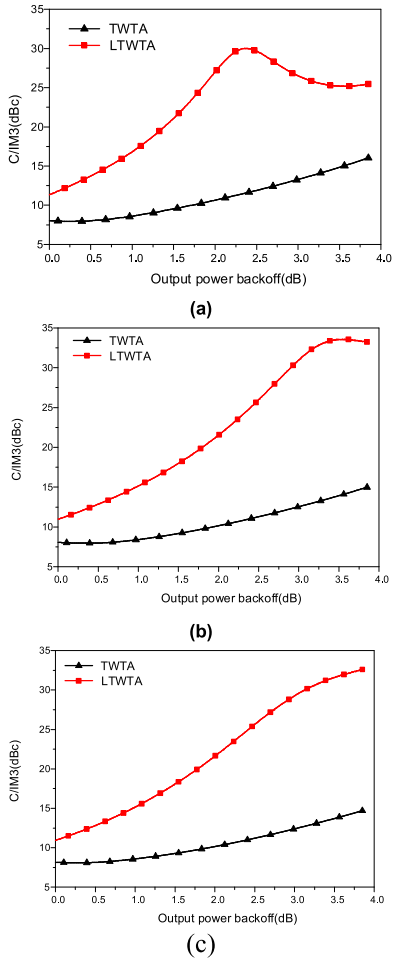

FIGURE 16. Measured two-tone IM3 of TWTA and LTWTA (a) 17GHz, (b) 18.5GHz and (c) 20GHz.

TWTA and linearized TWTA. Phase change of LTWTA is reduced from to 48° to 6.5°.

Measured C/IM3 of TWTA and LTWTA is shown in Fig. 16 and C/IM3 was measured with a 20 MHz spacing two- tone signal. C/IM3 increases from 14.2, 13.4 and 12.9 dBc to 25.5, 26.7 and 27.3 dBc at 17, 18.5 and 20 GHz in 3 dB OBO (output power back-off), respectively.

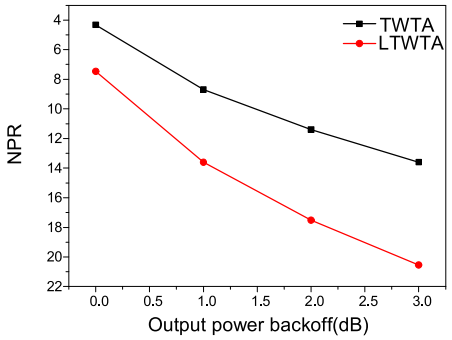

FIGURE 17. Measured NPR of the TWTA and linearized TWTA at 18.5 GHz.

Fig. 17 shows measured noise power ratio (NPR) in 80MHz frequency bandwidths of TWTA at 18.5 GHz, the NPR of TWTA increases from 13.6 dB to 20.56 dB. These results illustrate that the proposed APD can obviously improve the linearity of the TWTA.

Table 1 compares this work with other reported wideband APDs from the aspects of bandwidth, linearization effect and circuit complexity. The design in [7] shows good linear performance, but the structure using vector combination is complex. The design in [4] also shows good linear performance, but the technical information of APD is not mentioned. The design in [3] shows the ability of frequency-dependent phase conversion, but frequency-dependent gain conversion is not mentioned and the structure is complex. The proposed wideband APD shows good linearization effect with a simpler structure.

IV. CONCLUSION

A design method of the APD, which can transform the complicated nonlinear circuit design to the IMN design, for wideband application have been reported in this letter. The design procedure for wideband application is to design the specify IMN terminal impedance curve varying with frequency. A wideband APD operating in K-band (17- 20GHz) is designed and fabricated. Then a 100W K-band TWTA is used to validate the performance of the fabricated wideband APD. The results show that the proposed design method is an effective and simple design guide for wideband APD.

REFERENCES

[1] A. Katz, J. Wood, and D. Chokola, "The evolution of PA linearization: From classic feedforward and feedback through analog and digital predistortion," *IEEE Microw. Mag.*, vol. 17, no. 2, pp. 32–40, Feb. 2016.

[2] Y.-S. Lee, M.-W. Lee, and Y.-H. Jeong, "A wideband analog predistortion power amplifier with multi-branch nonlinear path for memory-effect compensation," *IEEE Microw. Wireless Compon. Lett.*, vol. 19, no. 7, pp. 476–478, Jul. 2009.

[3] D. Zhang, X. Xu, H. Yu, J. Li, T. B. Kumar, K. Ma, and K. S. Yeo, "Predistortion linearizer for wideband AM/PM cancelation with left-handed delay line," *IEEE Microw. Wireless Compon. Lett.*, vol. 27, no. 9, pp. 794–796, Sep. 2017.

[4] A. Katz, R. Gray, and R. Dorval, "Linearizers for *Q*-and *V*-band TWTAs," *IEEE Trans. Electron Devices*, vol. 65, no. 6, pp. 2371–2377, Jun. 2018.

[5] X. Hu, G. Wang, Z.-C. Wang, and J.-R. Luo, "Predistortion linearization of an X-Band TWTA for communications applications," *IEEE Trans. Electron Devices*, vol. 58, no. 6, pp. 1768–1774, Jun. 2011.

[6] H. Deng, D. Zhang, D. Lv, D. Zhou, and Y. Zhang, "Analog predistortion linearizer with independently tunable gain and phase conversions for ka-band TWTA," *IEEE Trans. Electron Devices*, vol. 66, no. 3, pp. 1533–1539, Mar. 2019.

[7] J.-F. Villemazet, H. Yahi, B. Lefebvre, F. Baudeigne, J. Maynard, G. Soubercaze-Pun, and L. Lapierre, "New ka-band analog predistortion linearizer allowing a 2.9 GHz instantaneous wideband satellite operation," in *Proc. 47th Eur. Microw. Conf. (EuMC)*, Nuremberg, Germany, Oct. 2017, pp. 302–305.

[8] H. Deng, D. Zhang, D. Lv, D. Zhou, and Y. Zhang, "A tunable reflective analog predistorter based on variable impedance matching network," *AEU-Int. J. Electron. Commun.*, vol. 98, pp. 139–143, Jan. 2019.

[9] Q. Cai, W. Che, K. Ma, and M. Zhang, "A simplified transistor-based analog predistorter for a GaN power amplifier," *IEEE Trans. Circuits Syst. II: Exp. Briefs*, vol. 65, no. 3, pp. 326–330, Mar. 2018.

[10] G. C. Tripathi and M. Rawat, "RFin–RFout linearizer system design for satellite communication," *IEEE Trans. Electron Devices*, vol. 65, no. 6, pp. 2378–2384, Jun. 2018.

[11] M. S. Hashmi, Z. S. Rogojan, and F. M. Ghannouchi, "A flexible dual-inflection point RF predistortion linearizer for microwave power amplifiers," in *Proc. Prog. Electromagn. Res. Conf.*, vol. 13, 2010, pp. 1–18.

CHENGE BIAN was born in 1996. He received the B.S. degree in information engineering from Xi'an Jiaotong University, Xi'an, China, in 2018. He is currently pursuing the M.S. degree with the National Digital Switching System Engineering and Technological Research Center, Zhengzhou, China. His current research interests include power amplifier linearization and passive components.

DEWEI ZHANG received the Ph.D. degree from the National Digital Switching System Engineering and Technological Research Center, Zhengzhou, China, in 2005. He is currently working with the National Digital Switching System Engineering and Technological Research Center. His current research interests include RF/microwave devices, such as antennas, filters and power amplifier, for wireless communications, and radar systems.

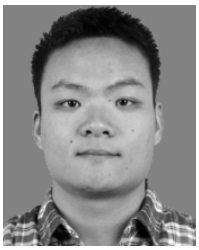

HAILIN DENG was born in 1992. He received the M.S. degree from the Zhengzhou Institute of Science and Information Technology Engineering, Zhengzhou, China, in 2016. He is currently pursuing the Ph.D. degree with the National Digital Switching System Engineering and Technology Research and Development Center, Zhengzhou.

His current research interests include power amplifier linearization and metamaterials.

DALONG LV received the Ph.D. degree from the National Digital Switching System Engineering and Technological Research Center, Zhengzhou, China, in 2013.

He is currently working with the National Digital Switching System Engineering and Technological Research Center. His current research interests include RF/microwave devices, such as antennas, filters, and power amplifier.

YI ZHANG received the Ph.D. degree in electronic engineering from Tsinghua University, Beijing, China, in 2015. He is currently working with the National Digital Switching System Engineering and Technological Research Center, Zhengzhou, China. His current research interests include microwave passive components, antennas, and electromagnetic metamaterials and devices.